

NO-H192 568

ANOMALIES IN THE HEAT-CAPACITY SIGNATURES OF
SUBMONOLAYER ADSORBATES WITH ATTRACTIVE LATERAL
INTERACTIONS(U) ROCHESTER UNIV NY DEPT OF CHEMISTRY

1/1

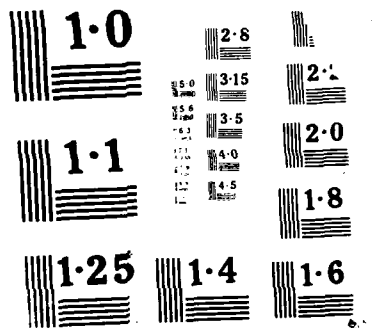
UNCLASSIFIED

Y S KIM ET AL

F/G 28/13

NL





DISTRIBUTION STATEMENT A

Approved for public release
Distribution Unlimited

ANOMALIES IN THE HEAT-CAPACITY SIGNATURES OF SUBMONOLAYER ADSORBATES WITH
ATTRACTIVE LATERAL INTERACTIONS

Young Sik Kim[†]
Department of Chemistry
University of Rochester
Rochester, New York 14627

Franco Battaglia* and Thomas F. George
Departments of Physics & Astronomy and Chemistry
239 Fronczak Hall
State University of New York at Buffalo
Buffalo, New York 14260

Abstract

The analytic closed form of the heat-capacity signatures previously derived for the McQuistan-Hock (MQH) model of a lattice gas is applied to various adsorbed systems for which the lateral interaction varies from a few meV to about 300 meV. It is shown that whenever the adsorption system can be described by a two-dimensional gas on which the substrate effects are less important than the adatom-adatom interactions, the computed temperatures at which the heat-capacity signatures display their maximum are in excellent agreement with the experimental measurements.

[†]Present address: Departments of Physics & Astronomy and Chemistry
239 Fronczak Hall
State University of New York at Buffalo
Buffalo, New York 14260

* Permanent address: Dipartimento di Chimica
Università della Basilicata
85100 Potenza, Italy

Accession For	
NTIS CRA&I	
DTIC TAB	
Unannounced	
Justification	
By	
Distribution	
Availability Code	
Dist	Availability Code
A-1	

88 217 006

I. Introduction

Recently McQuistan and Hock¹ have developed an exact solution for the distribution function of q indistinguishable particles on a $2 \times N$ lattice, where N is a positive integer. In a previous paper² (hereafter called paper I), we have derived an analytic closed form for the heat-capacity signatures from the McQuistan-Hock (MQH) model and have tested the model by comparing our computed temperatures T_c at which the heat capacity displays its maximum value with experimental measurements on Ne, Ar and Xe adsorbed on graphite, and with some other model calculations. In spite of its simplicity and its being an almost one-dimensional model, the MQH model gave for these systems good predictions for the temperatures at which the heat-capacity signatures display their anomaly. For instance, denoting by R the ratio between T_c and the interaction strength $|V_{11}|$ among two nearest-neighbor occupied pairs, the one-dimensional Ising model,³ the MQH model² and the average experimental measurements for Ne, Ar and Xe on graphite give for R the values of 0.21, 0.43 and 0.46, respectively. The MQH model obviously represents a logical extension from a one-dimensional to the more realistic full two-dimensional representation of the physical situation.

One might wonder about the justification of even considering a $2 \times N$ model given that there are excellent numerical techniques for finding with well-controlled accuracy the solution to the full two-dimensional problem. The justification resides in the very fact that in going from the one-dimensional model to the $2 \times N$ one, there is an abrupt significant improvement in the predictions of the experiments as far as the T_c 's are concerned. This implies not only that moving to the $N \times N$ model should not improve the results significantly, but also and more importantly, that most of the physics of the liquid-vapor equilibrium in two-dimensions is already in the $2 \times N$ quasi-one-dimensional model. Actually, as we shall see, the model describes only a limited

portion of the full phase diagram of a two-dimensional system, namely, the one relative to the liquid-vapor equilibrium. Furthermore, the model has the advantage of being exactly solvable and containing very few parameters, namely V_{11} , V_0 (the interaction strength between an adparticle and its own site) and V_{00} (the interaction strength between two vacant nearest-neighbor sites). This latter parameter might turn out to be quite valuable in that it accounts for distortion of the substrate, an effect that has been invoked by various authors⁴⁻⁶ to explain some details of the experimental heat-capacity signatures. Due to the remarkable agreement between the experimental values of T_c and the ones calculated from the MQH model for the systems we have made our test, we have been encouraged to apply the model to a wider variety of systems so as to scan a greater number of experimental data. Our choices have been limited only by the availability of accurate estimates of the interaction strengths and accurate experimental heat-capacity signatures. In particular, we have considered Kr, CH₄ and O₂ on graphite, and Cu, Ag, Au, Ni and Pd on tungsten. In the next section we review briefly the MQH model in connection with the computation of heat-capacity signatures. In the third and last section we present and discuss our results.

II. Theory

The theory of the $2 \times N$ lattice has been extensively described in detail in Ref. 1 and its application to the computation of heat-capacity signatures in Ref. 2 (paper I). In this section we give only the relevant results. In order to study the behavior of the heat capacity as a function of temperature, keeping the spreading pressure p and the number of adparticles q as constant, it is most convenient to work within the isothermal-isobaric ensemble, whose partition

function for a system of q indistinguishable particles on a $2 \times N$ lattice is given by

$$\Delta(q, \beta, p) = \tau^q \sum_{N=1}^{\infty} f_N(q, \beta) \eta^N, \quad (1)$$

where $\eta = e^{-2\beta p}$, $\tau = e^{-\beta V_0}$, and β^{-1} is the temperature times the Boltzmann constant k_B . In Eq. (1),

$$f_N(q, \beta) = \sum_{n_{00}} \sum_{n_{11}} A(N, q, n_{00}, n_{11}) x^{n_{11}} y^{n_{00}}, \quad (2)$$

where $x \equiv e^{-V_{11}\beta}$ and $y \equiv e^{-V_{00}\beta}$. The number of unique ways q indistinguishable particles can be arranged on a rectangular $2 \times N$ lattice to form n_{11} occupied nearest-neighbor pairs and n_{00} vacant nearest-neighbor pairs is given by $A(N, q, n_{00}, n_{11})$ by making use of a 15-term recursion relation.¹ In paper I we have shown that $\Delta(q, \beta, p)$ can be written as

$$\Delta_q = \sum_{j=1}^3 x(z_j) z_j^{-q}, \quad 0 < q \leq 2N \quad (3)$$

where the z_j 's are the solutions of the equation

$$1 + D_1 z + D_2 z^2 + D_3 z^3 = 0 \quad (4)$$

and

$$x(z) = - \frac{c_0 + c_1 z + c_2^2 z}{D_1 + 2D_2 z + 3D_3 z^2} \quad (5)$$

In Eqs. (4) and (5) the coefficients are defined as follows ($j = 1, 2, 3$):

$$d_0^2 c_j = c_{j+1} d_0 - c_0 d_{j+1} \quad (6)$$

$$D_j = d_j / d_0 \quad (7)$$

where

$$c_0 = y\eta \quad (8a)$$

$$c_1 = \eta\tau[2d_0 + y\eta(4y - xy - 1)] \quad (8b)$$

$$c_2 = \eta\tau^2[xd_0 + xy\eta(2-x^2)] \quad (8c)$$

$$c_3 = x\eta^2\tau^3\{[x^2y\eta + 4y\eta(1-x)](xy-1) + (4 - y - 2x)(x - xy^3\eta + y^2\eta) - 1\} \quad (8d)$$

$$d_0 = 1 - y^3\eta \quad (9a)$$

$$d_1 = -\eta(xy d_0 + y^3\eta + 1)\tau \quad (9b)$$

$$d_2 = -\eta(x^3 d_0 + xy\eta)\tau^2 \quad (9c)$$

$$d_3 = x\eta^2(xy-1)[x^2d_0 + y\eta(2xy-1)]t^3 \quad (9d)$$

From $\Delta(q, \beta, p)$, the heat capacity is given by

$$C(q, \beta, p) = k_B \beta^2 \left[\frac{\Delta''}{\Delta} - \left(\frac{\Delta'}{\Delta} \right)^2 \right] \quad (10)$$

where the prime denotes the derivative with respect to β ; the value $\beta_c = (k_B T_c)^{-1}$ at which $C(q, \beta, p)$ exhibits its maximum is given by the solution of the equation

$$2\Delta(\Delta')^2 + 3\beta\Delta\Delta'\Delta'' - 2\beta(\Delta')^3 - \beta\Delta^2\Delta'' - 2\Delta^2\Delta''' = 0 \quad (11)$$

III. Results and Discussion

The MQH model contains very few parameters, namely V_0 , V_{00} and V_{11} ; yet those parameters are apparently sufficient to determine the "gross" features of the statistics of adsorption. In this paper we are interested at the simulation of the critical temperatures as determined by the heat-capacity signatures. Since the effect of V_{00} is expected to be small and since there is no reliable estimate for it, we have chosen $V_{00} \equiv 0$, which is equivalent to assuming a "rigid" lattice in which there is no interaction between two nearest-neighbor vacant sites. This is the same choice made by Hock and McQuistan in their computation of adsorption isotherms.⁷ Moreover, as can be seen from Eqs. (1), (3), (4), (9) and (10), although the partition function and the Gibbs free energy do depend on V_0 , the heat capacity, $C(q, \beta, p)$ in the thermodynamic limit does not. The role of the substrate is analogous to that of a third body in the description of the interaction between two particles embedded in a three-dimensional medium, and the only task the substrate accomplishes is to force the adsorbed particles onto a plane. The all-important parameter here is V_{11} , i.e., the interaction

strength between two occupied pairs, whose value is, of course, different than the free-space value. For Kr and CH_4 we refer to the results obtained by Cole and coworkers^{8,9} which are, to our knowledge, the most reliable data available. Their value of $|V_{11}| = 170$ K for Kr is in remarkable agreement with Putnam's¹⁰ value of 171 K. For CH_4 we take the value of $|V_{11}| = 177$ K. Another widely-studied system is two-dimensional oxygen adsorbed on graphite. It has been investigated experimentally¹¹ with use of heat capacity measurements, and calculations have been performed on it especially by Etters and coworkers.¹² These authors have used (and so do we) the estimate by English and Venables¹³ for $|V_{11}|$, i.e., 54 K. All systems mentioned so far, together with the ones studied in paper I, are adsorbed systems with a lateral interaction of the order of 10 meV. Recently, Kolaczkiewicz and Bauer¹⁴ have studied chemisorbed layers of metals (Cu, Ag, Au, Ni and Pd) for which thermal desorption spectroscopy measurements have shown that their desorption energies from W[100] surfaces increase with coverage, implying that the lateral interactions which are on the order of 300 meV are attractive. We shall compare our results for this range of adatom-adatom interactions with the ones of Kolaczkiewicz and Bauer, thereby showing that the MQH model has in fact a wide range of applicability.

Critical temperatures for the mentioned systems have been determined by various techniques, especially from heat capacity signatures,¹⁵⁻²¹ high-resolution synchrotron X-ray^{22,23} and low energy electron²⁴ diffraction studies, thermal desorption spectroscopy,^{25,26} and from the temperature dependence of the work function of adsorbate-covered surfaces.²⁷ As shown in the previous section, we are able to extract from the MQH series expansion for the canonical partition function, (Eq. (21)), a closed analytic form for the isothermal-isobaric partition function (Eq. (3)) from which one can compute heat-capacity signatures, (Eq. (10)) whose maximum is exhibited at the temperature T_c that solves Eq. (11).

In the MQH model the dependence of T_c on V_{11} is essentially linear with a slope that depends smoothly on the coverage θ (in particular, in the range $0.2 < \theta < 0.7$, the slope varies between 0.37 and 0.44). In Figs. 1 and 2 we display T_c as a function of $|V_{11}|$ for two ranges of $|V_{11}|$, namely 0 - 300 K (Fig. 1) and 2000-4000 K (Fig. 2). To compare with data available from literature, we have chosen $\theta = 0.5$ for the systems on graphite and $\theta = 0.3$ for the ones on tungsten. With the exception of Kr and Xe, the agreement between the prediction from the MQH and the experimental values for the systems shown in Fig. 1 is very good. According to Dash,²⁸ one can distinguish between three temperature-dependent types of film growing: either three-dimensional bulk develops asymptotically from the two-dimensional system, or there is no film but cluster growth, or, after the first two or three monolayers, cluster growth begins. Clearly, systems for which the film grows monolayer after monolayer are suitable to be well simulated by a two-dimensional lattice-gas model such as the MQH one.

In order to understand why the model gives such excellent predictions for Ne, O_2 , Ar and CH_4 on graphite, but not for Kr and Xe, let us first recall that adsorbed systems whose two-dimensional space symmetry results from the two-dimensional space symmetry of the substrate surface by adding or subtracting symmetry elements are named commensurate, and that adsorbed structures whose symmetry is not related to that of the substrate are named incommensurate. In many cases the periodic substrate of the hexagonal basal surface of graphite is covered by a $\sqrt{3}$ structure, in which the centers of non-adjacent hexagons are preferred adsorption sites and form a triangular lattice. Whether an adsorbate has commensurate phases depends on its incompatibility i , defined as $i = (a-d) \times 100/d$, where a is the lattice constant of the $\sqrt{3}$ structure (4.263 Å for graphite³⁰) and d is the lattice constant of the [111]-plane of the adsorbate species in three-dimensional bulk (Ne, Ar, Kr, Xe, CH_4 and O_2 condense into the

cubic system). For incompatibilities i positive and less than a substrate-dependent value i_0 , commensurate structures are energetically preferred. For graphite $i_0 \sim 5$, and the values of i for Ar, Kr, Xe and CH_4 on graphite are 14.6, 5.4, -2.8 and 1.6, respectively.^{29,30} Adsorbates in a commensurate phase cannot be properly described by a lattice-gas model such as the MQH one, in which the only role of the substrate is to constrain the adsorbate particles on a plane. In an incommensurate phase the adatom-adatom interaction dominates on the substrate influence, and the MQH model is expected to be well suited to simulate the heat-capacity anomalies corresponding to two-dimensional incommensurate phases.

From the above values of the incompatibilities and from the fact that there is no evidence³¹ of a commensurate phase for O_2 (for which the incompatibility value can be safely estimated to be $i \sim 10$), it is now clear why the MQH model gives an excellent prediction of the heat-capacity anomalies for O_2 and Ar, and a poor prediction for Kr. (Kr displays a commensurate-incommensurate phase transition^{32,33} but, in the range 70-130 K, it occurs at coverages greater than unity; Ar was found incommensurate at all conditions studied.^{34,35}) As already mentioned, CH_4 has a low value of incompatibility which might invalidate the above reasoning. This is not the case because the phase diagram of two-dimensional methane adsorbed on graphite¹⁵ shows a temperature-triggered commensurate-incommensurate transition at $T = 47$ K and coverages below 0.8 monolayers.³⁶ Therefore, the anomaly at $T = 75$ K occurs in a region where the adsorbate-adsorbate interactions play a major role.

This is also the case of Ne, as can be seen from the phase diagram proposed by Huff and Dash⁴ for submonolayers in the temperature range 1-20 K: melting occurs at 13.5 K, so that the anomaly at 16 K cannot involve any solid commensurate phase. (The barely stable $(\sqrt{7} \times \sqrt{7})\text{R}19^\circ$ structure exists only at

temperatures below 4 K.³⁷⁾ Xe has a negative incompatibility and is therefore expected to be highly mobile, because when the [111]-plane is isolated from the bulk, its lattice constant (that in bulk is already larger than the lattice constant of the $\sqrt{3}$ structure) becomes even larger and the incommensurate phase is generally more stable. However, xenon has already shown a peculiar behavior with its unusually high value of the ratio T_{2c}/T_{3c} in spite of its negative incompatibility.³⁰ This has suggested¹⁹ that some different mechanism of localization is causing the formation of a structure which is in registry with the solid substrate and with a positive value (11.6) of the incompatibility. Whatever the case might be, we point out that although the quantitative predictions from the MQH model for adsorbates whose structure is somehow reminiscent of the substrate structure are not as excellent as for adsorbates that are, without doubt, incommensurate to the substrate, the relative qualitative behavior is in agreement with the experimental findings, and the quantitative differences are not so serious in spite of the simplicity of the model. This is clearly shown for Kr on graphite and for the systems to be considered next.

In Fig. 2 we compare our results from the MQH model in a range of much stronger (200-300 meV) lateral interaction energies with systems for which accurate estimates of both adatom-adatom potentials and critical temperatures are available. Kolaczekiewicz and Bauer¹⁴ have filled a gap in the literature by studying chemisorbed layers with attractive lateral interactions. They have constructed from work function measurements the coexistence line of Cu, Ag, Au, Ni and Pd adsorbed on W[110], and have shown that at submonolayer coverages these systems can be described by a law of corresponding states in the form of a two-dimensional van der Waals equation (with a critical coverage at $\theta \approx 0.3$). From their adatom-adatom Lennard-Jones potential parameters, we estimate, taking into

account the harmonic zero-point energy correction ($\frac{6\pi}{\sigma} 2^{1/3} \sqrt{\epsilon/\mu}$), the interaction strength V_{11} (σ is the hard-core diameter of the adatom, ϵ is the well depth and μ is the reduced mass). This is displayed in Table 1 with the temperatures T_c calculated from the MQH model and estimated from a van der Waals fitting of the experimental data. Again we can see that the qualitative behavior of T_c as computed from the MQH model is in agreement with available data from the literature, even in the region of strong lateral interactions. The van der Waals fitting performed by Kolaczkiwicz and Bauer on their experimental data gives interaction strengths that, when used in the MQH model, give back the experimental T_c trend. Quantitatively, the results are not as satisfactory as for Ne, Ar, O_2 and CH_4 on graphite. We cannot ascribe the discrepancies to a bad estimate of the adatom-adatom interaction strength that, for the systems on tungsten, has not been determined as accurately as for the systems on graphite. On the contrary, we expect that V_{11} as given in Table I is an upper bound to the real value, thereby giving a less satisfactory result for T_c . Again, the reason for this has to be found in the structural properties of these metal layers on tungsten surfaces: the lateral periodicity of the adsorbate is very close²⁶ (if not identical) to that of the substrate whose effects on the T_c 's are not taken into account by the MQH model.

In Fig. 3 we show the two-dimensional phase diagram which can be obtained within the limits of the MQH model. The displayed curve divides the plane into two regions that are very much reminiscent of the liquid-vapor equilibrium of the bulk phase. Compared with available experimental data of chemisorbed metals on tungsten, we find that: (1) the critical coverage ($\theta_c \approx 0.8$) in the MQH model is much larger than the experimental results ($\theta_c \approx 0.3$), and (2) the ratios $-T_c/V_{11}$ for chemisorbed metals are larger than those from the MQH model.² Since this model contains only the interaction strength between two occupied pairs (V_{11}), it

does not take into account the adparticle size as well as substrate effects. If we assume the simple Lennard-Jones pairwise interaction potential between adparticles and fix the monolayer density, then θ_c is inversely proportional to the hard-core diameter σ of the adatom. Thus, the MQH model, which neglects the size of the adatom, will give large values for the critical coverage. Also, the adatoms are bound more strongly to the substrate atoms than to themselves, so that fewer electrons are available for lateral bonding. The strong adatom-substrate interaction reduces V_{11} , which in turn increases the ratio $-T_c/V_{11}$. We should further mention that at very low and at high coverages the model might fail because of the substrate inhomogeneity and because of multilayer effects, respectively.

In conclusion, the MQH model is very appealing for describing heat-capacity anomalies of adsorbate-substrate systems, provided (i) no solid commensurate phase is involved in the region around T_c , (ii) the pairwise interaction V_{11} among nearest-neighbor adparticles is the parameter that plays the major role in transition process, with only lower-order effects due to the substrate, and (iii) the transition is not of first order. These conditions are not very restrictive, and moreover, they are not independent because very often the first one implies the second, as has been already discussed, and in many instances also the third one, since several transitions from or into commensurate phases have been predicted to be of first order.³⁸

Acknowledgments

This research was supported by National Science Foundation under Grant CHE-8620274, the Air Force Office of Scientific Research (AFSC), United States Air Force, under Contract F49620-86-C-0009, and the Office of Naval Research. The United States Government is authorized to reproduce and distribute reprints

notwithstanding any copyright notation hereon. FB acknowledges the Italian CNR for financial support.

References

1. R. B. McQuistan and J. L. Hock, J. Math. Phys. 25, 261 (1984).
2. F. Battaglia, Y. S. Kim and T. F. George, J. Phys. Chem. 91, 414 (1987).
3. T. L. Hill, Statistical Mechanics (McGraw-Hill, New York, 1956), Ch. 7.
4. G. B. Huff and J. G. Dash, J. Low Temp. Phys. 24, 155 (1976).
5. R. E. Rapp, E. P. De Souza and E. Lerner, Phys. Rev. B 24 2196 (1981).
6. S. C. Ying, J. Vac. Sci. Technol. 18, 500 (1981).
7. J. L. Hock and R. B. McQuistan, J. Math. Phys. 26, 2392 (1985).
8. J. R. Klein and M. W. Cole, Faraday Discuss. Chem. Soc. 80, 71 (1985).
9. S. Rauber, J. R. Klein and M. W. Cole, Phys. Rev. B 27, 1314 (1983).
10. F. A. Putnam, in Ordering in Two Dimensions, ed. by S. K. Sinha (North-Holland, Amsterdam, 1980), p. 231.
11. R. Marx and R. Braun, Solid State Commun. 33, 229 (1980).
12. R. D. Etters, Ru-Pin Pan and V. Chandrasekharan, Phys. Rev. Lett. 45, 645 (1980).
13. C. A. English and J. A. Venables, Proc. Roy. Soc. London A 340, 57 (1974).
14. J. Kolaczkiwicz and E. Bauer, Surf. Sci. 151, 333 (1985).
15. R. Marx and E. F. Wassermann, Surf. Sci. 117, 267 (1982).
16. R. Marx, Phys. Rep. 125, 1 (1985).
17. A. Thomy and X. Duval, J. Chim. Phys. 67, 1101 (1970).
18. A. Thomy and X. Duval, Carbon 13, 242 (1974).
19. Y. Larher, J. Chem. Soc. Faraday Trans. I 70, 320 (1974).
20. Y. Larher and B. Gilquin, Phys. Rev. A 20, 1599 (1979).
21. T. T. Chung, Surf. Sci. 87, 348 (1979).

22. M. Nielsen, J. Als-Nielsen, J. Bohr and J. P. McTague, Phys. Rev. Lett. 47, 582 (1981).
23. J. P. McTague, J. Als-Nielsen, J. Bohr and M. Nielsen, Phys. Rev. B 25, 7765 (1982).
24. J. M. Gay, A. Dutheil, J. Krim and J. Suzanne, Surf. Sci. 177, 25 (1986).
25. E. Bauer, F. Bonczek, H. Poppa and G. Todd, Surf. Sci. 53, 87 (1975).
26. E. Schlenk and E. Bauer, Surf. Sci. 93, 9 (1980).
27. J. Kolaczkiwicz and E. Bauer, Phys. Rev. Lett. 53, 485 (1984).
28. J. G. Dash, Phys. Rev. B 15, 3136 (1977).
29. A. Patrykiewicz, Thin Solid Films 76, 241 (1981).
30. C. Tessier and Y. Larher, in Ordering in Two Dimensions, ed. by S. K. Sinha (North-Holland, Amsterdam, 1980), p. 163.
31. M. Nielsen and J. P. McTague, Phys. Rev. B 19, 3096 (1979).
32. R. J. Birgenau, E. M. Hammons, P. Heiney, P. W. Stephens and P. M. Hoth, in Ordering in Two Dimensions, ed. by S. K. Sinha (North-Holland, Amsterdam, 1980), p. 29.
33. A. Thomy, X. Duval and J. Regnier, Surf. Sci. Rep. 1, 1 (1981).
34. H. Taub, K. Carneiro, J. K. Kjems, L. Passal and J. P. McTague, Phys. Rev. B 16, 4551 (1977).
35. H. Taub, L. Passal, J. K. Kjems, K. Corneiro, J. P. McTague and J. G. Desh, Phys. Rev. Lett. 34, 654 (1975).
36. R. Marx, Z. Phys. B 46, 237 (1982).
37. H. Wiechert, C. Tiby and H. J. Lauter, Physica B 108, 785 (1981).
38. E. Domany, M. Schick and J. S. Walker, Phys. Rev. Lett. 38, 1148 (1977).

Table I

Computed (T_c) and experimental (T_{Exp}) critical temperatures of Ne, Ar, Kr, Xe, O_2 and CH_4 on graphite (coverage $\theta = 0.5$) and Cu, Ag, Au, Ni and Pd on W[110] (coverage $\theta = 0.3$). V_{11} are the adatom-adatom interaction strengths. All data are in Kelvin.

	$-V_{11}^a)$	T_c	$T_{Exp}^b)$
Ne	35	15	16
Ar	120	51	50
Kr	170	71	85
Xe	236	102	118
O_2	54	23	25
CH_4	177	75	75
Cu	2850	1120	1170
Ag	2360	927	980
Au	2910	1143	1130
Ni	3430	1348	1400
Pd	2900	1140	1170

a) Taken from Refs. 8 and 9 for Ne, Ar, Kr, Xe and CH_4 , from Refs. 12 and 13 for O_2 , and from Ref. 14 for Cu, Ag, Au, Ni and Pd.

b) Taken from Ref. 8 for Ne, Xe and CH_4 , from Ref. 21 for Ar, from Refs. 18-20 for Kr, from Ref. 16 for O_2 , from Ref. 14 for Cu, Ag, Ni and Pd, and from Ref. 27 for Au.

Figure Captions

1. The solid line shows critical temperatures T_c from the MQH model as a function of the adatom-adatom interaction strength V_{11} , in the range 0-30 meV. Circles represent available data for some adparticles on graphite.
2. The solid line shows critical temperature T_c from the MQH model as a function of the adatom-adatom strength V_{11} in the range 150-350 meV. Circles represent results from Ref. 14.
3. Phase diagram from the MQH model. Solid line: model phase boundary; ★:Cu, ▲:Ni, •:Ag, □:Pd, +:Au on W(110) from experimental data (Ref. 14).

Fig. 1

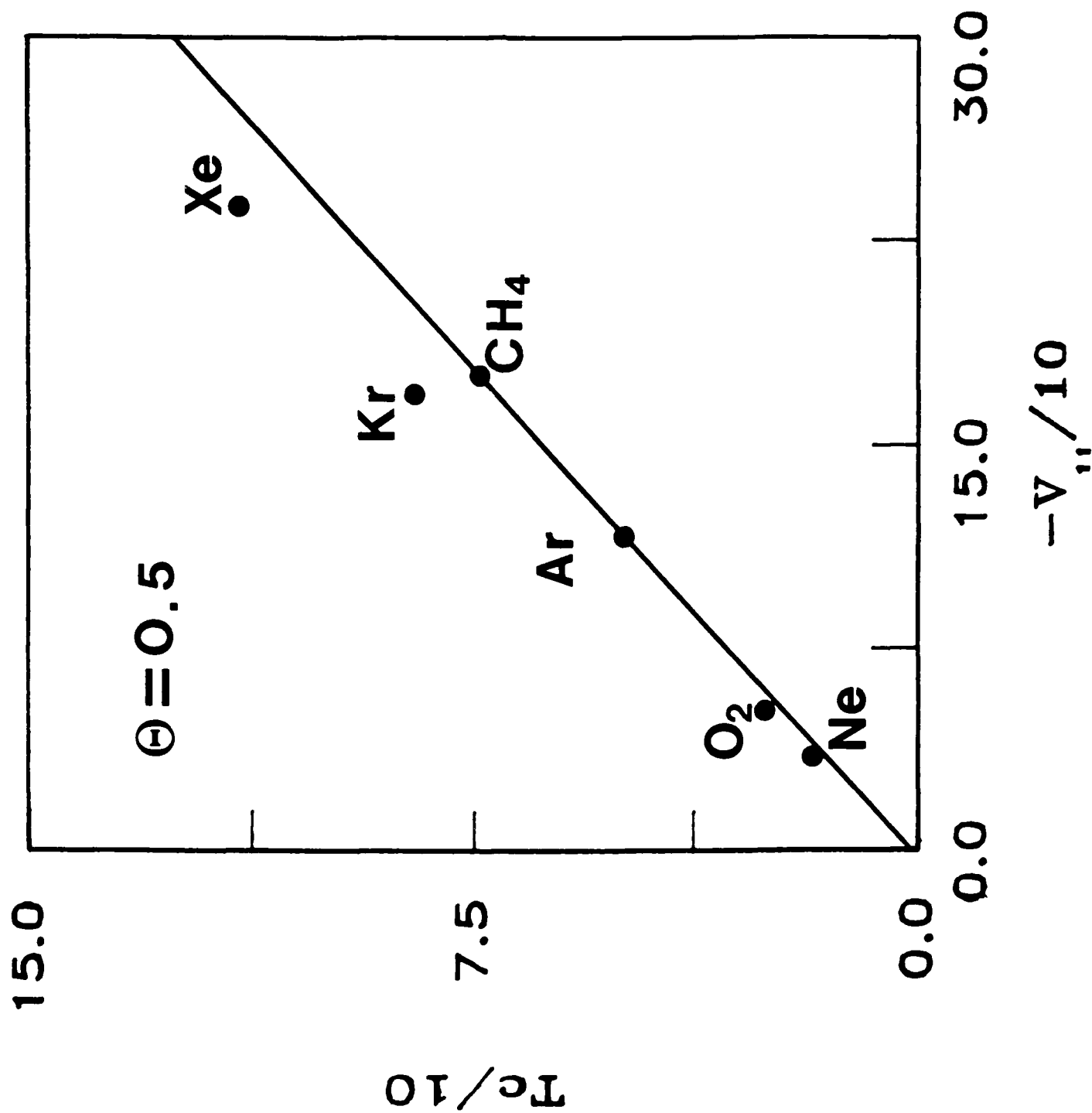


Fig. 2

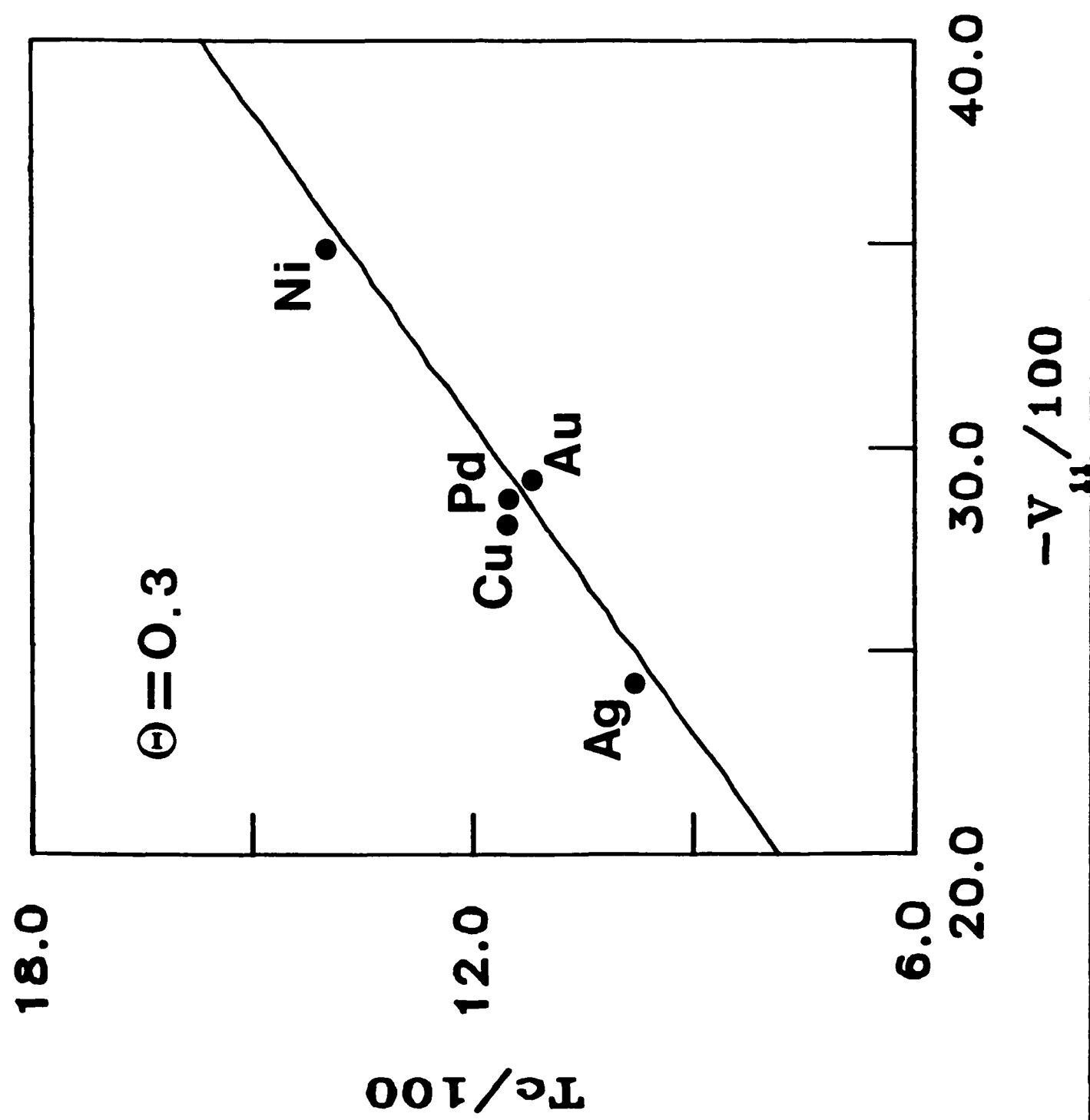
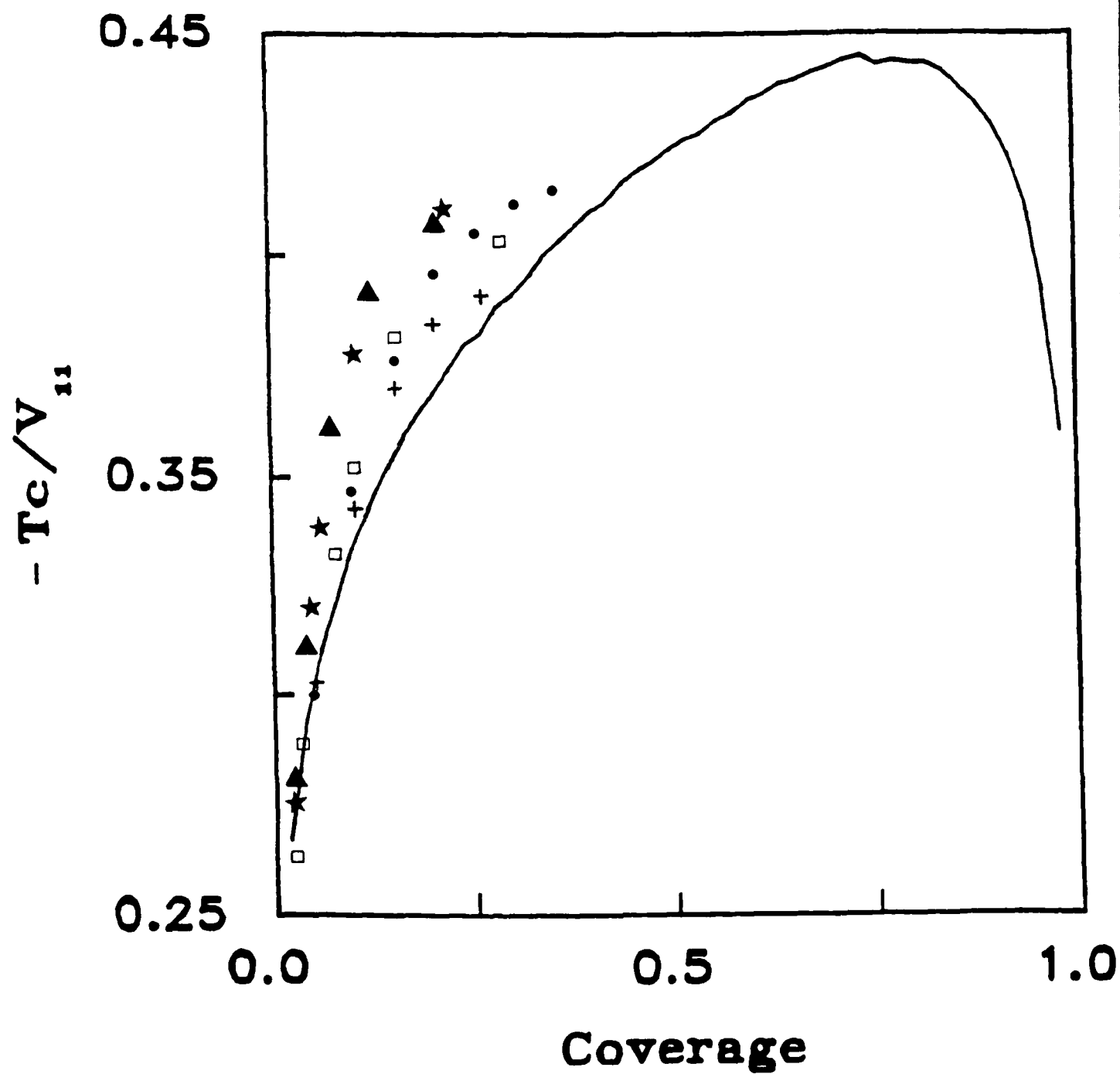


Fig. 3



TECHNICAL REPORT DISTRIBUTION LIST, GEN

	<u>No. Copies</u>		<u>No. Copies</u>
Office of Naval Research Attn: Code 1113 800 N. Quincy Street Arlington, Virginia 22217-5000	2	Dr. David Young Code 334 NORDA NSTL, Mississippi 39529	1
Dr. Bernard Douda Naval Weapons Support Center Code 50C Crane, Indiana 47522-5050	1	Naval Weapons Center Attn: Dr. Ron Atkins Chemistry Division China Lake, California 93555	1
Naval Civil Engineering Laboratory Attn: Dr. R. W. Drisko, Code L52 Port Hueneme, California 93401	1	Scientific Advisor Commandant of the Marine Corps Code RD-1 Washington, D.C. 20380	1
Defense Technical Information Center Building 5, Cameron Station Alexandria, Virginia 22314	12 high quality	U.S. Army Research Office Attn: CRD-AA-IP P.O. Box 12211 Research Triangle Park, NC 27709	1
DTNSRDC Attn: Dr. H. Singerman Applied Chemistry Division Annapolis, Maryland 21401	1	Mr. John Boyle Materials Branch Naval Ship Engineering Center Philadelphia, Pennsylvania 19112	1
Dr. William Tolles Superintendent Chemistry Division, Code 6100 Naval Research Laboratory Washington, D.C. 20375-5000	1	Naval Ocean Systems Center Attn: Dr. S. Yamamoto Marine Sciences Division San Diego, California 92132	1
		Dr. David L. Nelson Chemistry Division Office of Naval Research 800 North Quincy Street Arlington, Virginia 22217	1

ABSTRACTS DISTRIBUTION LIST, 056/625/629

Dr. J. E. Jensen
Hughes Research Laboratory
3011 Malibu Canyon Road
Malibu, California 90265

Dr. C. B. Harris
Department of Chemistry
University of California
Berkeley, California 94720

Dr. J. H. Weaver
Department of Chemical Engineering
and Materials Science
University of Minnesota
Minneapolis, Minnesota 55455

Dr. F. Kutzler
Department of Chemistry
Box 5055
Tennessee Technological University
Cookeville, Tennessee 38501

Dr. A. Reisman
Microelectronics Center of North Carolina
Research Triangle Park, North Carolina
27709

Dr. D. DiLella
Chemistry Department
George Washington University
Washington D.C. 20052

Dr. M. Grunze
Laboratory for Surface Science and
Technology
University of Maine
Orono, Maine 04469

Dr. R. Reeves
Chemistry Department
Rensselaer Polytechnic Institute
Troy, New York 12181

Dr. J. Butler
Naval Research Laboratory
Code 6115
Washington D.C. 20375-5000

Dr. Steven M. George
Stanford University
Department of Chemistry
Stanford, CA 94305

Dr. L. Interante
Chemistry Department
Rensselaer Polytechnic Institute
Troy, New York 12181

Dr. Mark Johnson
Yale University
Department of Chemistry
New Haven, CT 06511-8118

Dr. Irvin Heard
Chemistry and Physics Department
Lincoln University
Lincoln University, Pennsylvania 19352

Dr. W. Knauer
Hughes Research Laboratory
3011 Malibu Canyon Road
Malibu, California 90265

Dr. K.J. Klaubunde
Department of Chemistry
Kansas State University
Manhattan, Kansas 66506

ABSTRACTS DISTRIBUTION LIST, 056/625/629

Dr. G. A. Somorjai
Department of Chemistry
University of California
Berkeley, California 94720

Dr. J. Murday
Naval Research Laboratory
Code 6170
Washington, D.C. 20375-5000

Dr. J. B. Hudson
Materials Division
Rensselaer Polytechnic Institute
Troy, New York 12181

Dr. Theodore E. Madey
Surface Chemistry Section
Department of Commerce
National Bureau of Standards
Washington, D.C. 20234

Dr. J. E. Demuth
IBM Corporation
Thomas J. Watson Research Center
P.O. Box 218
Yorktown Heights, New York 10598

Dr. M. G. Lagally
Department of Metallurgical
and Mining Engineering
University of Wisconsin
Madison, Wisconsin 53706

Dr. R. P. Van Duyne
Chemistry Department
Northwestern University
Evanston, Illinois 60637

Dr. J. M. White
Department of Chemistry
University of Texas
Austin, Texas 78712

Dr. D. E. Harrison
Department of Physics
Naval Postgraduate School
Monterey, California 93940

Dr. R. L. Park
Director, Center of Materials
Research
University of Maryland
College Park, Maryland 20742

Dr. W. T. Peria
Electrical Engineering Department
University of Minnesota
Minneapolis, Minnesota 55455

Dr. Keith H. Johnson
Department of Metallurgy and
Materials Science
Massachusetts Institute of Technology
Cambridge, Massachusetts 02139

Dr. S. Sibener
Department of Chemistry
James Franck Institute
5640 Ellis Avenue
Chicago, Illinois 60637

Dr. Arnold Green
Quantum Surface Dynamics Branch
Code 3817
Naval Weapons Center
China Lake, California 93555

Dr. A. Wold
Department of Chemistry
Brown University
Providence, Rhode Island 02912

Dr. S. L. Bernasek
Department of Chemistry
Princeton University
Princeton, New Jersey 08544

Dr. W. Kohn
Department of Physics
University of California, San Diego
La Jolla, California 92037

ABSTRACTS DISTRIBUTION LIST, 056/625/629

Dr. F. Carter
Code 6170
Naval Research Laboratory
Washington, D.C. 20375-5000

Dr. Richard Colton
Code 6170
Naval Research Laboratory
Washington, D.C. 20375-5000

Dr. Dan Pierce
National Bureau of Standards
Optical Physics Division
Washington, D.C. 20234

Dr. R. Stanley Williams
Department of Chemistry
University of California
Los Angeles, California 90024

Dr. R. P. Messmer
Materials Characterization Lab.
General Electric Company
Schenectady, New York 22217

Dr. Robert Gomer
Department of Chemistry
James Franck Institute
5640 Ellis Avenue
Chicago, Illinois 60637

Dr. Ronald Lee
R301
Naval Surface Weapons Center
White Oak
Silver Spring, Maryland 20910

Dr. Paul Schoen
Code 6190
Naval Research Laboratory
Washington, D.C. 20375-5000

Dr. John T. Yates
Department of Chemistry
University of Pittsburgh
Pittsburgh, Pennsylvania 15260

Dr. Richard Greene
Code 5230
Naval Research Laboratory
Washington, D.C. 20375-5000

Dr. L. Kesmodel
Department of Physics
Indiana University
Bloomington, Indiana 47403

Dr. K. C. Janda
University of Pittsburgh
Chemistry Building
Pittsburg, PA 15260

Dr. E. A. Irene
Department of Chemistry
University of North Carolina
Chapel Hill, North Carolina 27514

Dr. Adam Heller
Bell Laboratories
Murray Hill, New Jersey 07974

Dr. Martin Fleischmann
Department of Chemistry
University of Southampton
Southampton SO9 5NH
UNITED KINGDOM

Dr. H. Tachikawa
Chemistry Department
Jackson State University
Jackson, Mississippi 39217

Dr. John W. Wilkins
Cornell University
Laboratory of Atomic and
Solid State Physics
Ithaca, New York 14853

ABSTRACTS DISTRIBUTION LIST, 056/625/629

Dr. R. G. Wallis
Department of Physics
University of California
Irvine, California 92664

Dr. D. Ramaker
Chemistry Department
George Washington University
Washington, D.C. 20052

Dr. J. C. Hemminger
Chemistry Department
University of California
Irvine, California 92717

Dr. T. F. George
Chemistry Department
University of Rochester
Rochester, New York 14627

Dr. G. Rubloff
IBM
Thomas J. Watson Research Center
P.O. Box 218
Yorktown Heights, New York 10598

Dr. Horia Metiu
Chemistry Department
University of California
Santa Barbara, California 93106

Dr. W. Goddard
Department of Chemistry and Chemical
Engineering
California Institute of Technology
Pasadena, California 91125

Dr. P. Hansma
Department of Physics
University of California
Santa Barbara, California 93106

Dr. J. Baldeschwieler
Department of Chemistry and
Chemical Engineering
California Institute of Technology
Pasadena, California 91125

Dr. J. T. Keiser
Department of Chemistry
University of Richmond
Richmond, Virginia 23173

Dr. R. W. Plummer
Department of Physics
University of Pennsylvania
Philadelphia, Pennsylvania 19104

Dr. E. Yeager
Department of Chemistry
Case Western Reserve University
Cleveland, Ohio 44106

Dr. N. Winograd
Department of Chemistry
Pennsylvania State University
University Park, Pennsylvania 16802

Dr. Roald Hoffmann
Department of Chemistry
Cornell University
Ithaca, New York 14853

Dr. A. Steckl
Department of Electrical and
Systems Engineering
Rensselaer Polytechnic Institute
Troy, New York 12181

Dr. G.H. Morrison
Department of Chemistry
Cornell University
Ithaca, New York 14853

END

DATE

FILMED

DTIC

6-88